

Food & Function

Accepted Manuscript



This is an *Accepted Manuscript*, which has been through the Royal Society of Chemistry peer review process and has been accepted for publication.

Accepted Manuscripts are published online shortly after acceptance, before technical editing, formatting and proof reading. Using this free service, authors can make their results available to the community, in citable form, before we publish the edited article. We will replace this *Accepted Manuscript* with the edited and formatted *Advance Article* as soon as it is available.

You can find more information about *Accepted Manuscripts* in the [Information for Authors](#).

Please note that technical editing may introduce minor changes to the text and/or graphics, which may alter content. The journal's standard [Terms & Conditions](#) and the [Ethical guidelines](#) still apply. In no event shall the Royal Society of Chemistry be held responsible for any errors or omissions in this *Accepted Manuscript* or any consequences arising from the use of any information it contains.

1 **Protective Effects of Tartary Buckwheat Flavonoids on High TMAO Diet-Induced**
2 **Vascular Dysfunction and Liver Injury in Mice**

3

4 Yuanyuan Hu^a, Yan Zhao^{b,*}, Li Yuan^a, Xingbin Yang^{a,*}

5

6 ^aKey Laboratory of Ministry of Education for Medicinal Resource and Natural Pharmaceutical
7 Chemistry, College of Food Engineering and Nutritional Science, Shaanxi Normal University,
8 Xi'an 710062, China

9 ^bSchool of Pharmacy, Fourth Military Medical University, Xi'an 710032, China

10

11 *Corresponding author: Tel.: +86-29-85310517; fax: +86-29-85310517

12 E-mail address: xbyang@snnu.edu.cn (X.B. Yang), yanzhao@fmmu.edu.cn (Y. Zhao)

13 **Abstract**

14 This study was to investigate the liver and vascular changes in high trimethylamine-*N*-oxide
15 (TMAO) diet-fed mice, and the possible vasoprotective and hepatoprotective effects of purified
16 tartary buckwheat flavonoids fraction (TBF). HPLC analysis revealed that the content of rutin
17 and quercetin presented in TBF was 53.6% and 37.2%, respectively, accounting for 90.8% of
18 TBF. Mice fed 1.5% TMAO in drinking water for 8 weeks significantly displayed vascular
19 dysfunction and liver damage ($p < 0.01$). The administration of TBF at 400 and 800 mg/kg-bw
20 significantly elevated plasma NO and eNOS concentrations, and serum HDL-C and PGI₂ levels,
21 and lowered serum TC, TG, LDL-C, ET-1 and TX-A₂ levels of TMAO-fed mice. TBF also
22 reduced serum AST and ALT activities, and hepatic NEFA and MDA levels, and increased the
23 hepatic GSH-Px and SOD activities in TMAO-fed mice, which were consistent with the
24 observation of liver histological alteration. This report firstly showed that dietary TMAO might
25 cause liver damage and TBF prevented TMAO-induced vascular dysfunction and hepatic injury.

26 **Keywords:** TMAO, Tartary buckwheat, Vascular dysfunction, Liver injury, Protective effects

27 Introduction

28 Atherosclerosis is a major cause of cardiovascular disease (CVD), and endothelial
29 dysfunction is an early and independent predictor of most forms of CVD.¹ Damage to the
30 endothelium upsets the balance between vasoconstriction and vasodilation, which triggers or
31 exacerbates several CVD events including atherosclerosis.² Recently, plasma
32 trimethylamine-*N*-oxide (TMAO) was identified as a metabolite strongly associated with
33 atherosclerosis in a large case-control cohort for CVD.^{1,3} TMAO, an oxidation product of
34 trimethylamine (TMA), is a relatively common metabolite of nutrient choline and other
35 TMA-containing species (e.g. betaine, *L*-carnitine and lecithin) by gut microbiota.⁴ However,
36 the mechanism by which TMAO triggers atherosclerosis and increases cardiovascular risk is not
37 completely understood, but it has been reported that dietary supplementation of mice with
38 TMAO, choline or *L*-carnitine promotes up-regulation of multiple macrophage scavenger
39 receptors, such as CD36 and SRA1, both of which are involved in the uptake of modified
40 lipoproteins, which accelerates the build-up of arterial plaque and CVD.⁵ Furthermore, mice
41 supplemented with a diet rich in TMAO also exhibited a marked reduction (35%) in reverse
42 cholesterol transport (RCT).³ TMAO might additionally impact cholesterol metabolism via
43 decreasing bile acid synthesis, evidenced as a reduction of hepatic mRNA expression of the bile
44 acid synthesizing enzymes, *Cyp7a1* and *Cyp27a1*, in mice.^{3,5} For this reason, the potential
45 toxicological property of high TMAO diet and its toxic mechanism involved in vascular
46 endothelium damage need be further clarified.

47 Flavonoids comprise a large family of bioactive polyphenolic compounds found naturally in
48 herbs, fruits and vegetables with the benefits to modern chronic diseases.⁶⁻⁷ Despite the
49 established antioxidant and anti-inflammatory properties, flavonoids are also found to be
50 beneficial to CVD.⁸ Several biological mechanisms have been indicated to support a beneficial
51 effect of flavonoids on vascular endothelial function, suggesting a potential role of flavonoids in
52 improving arterial function and reducing the incidence of cardiovascular events.⁹⁻¹¹ However, to

53 our best knowledge, there are no available studies regarding the roles of natural dietary
54 flavonoids in the regulation of dietary TMAO-induced CVD, including vascular endothelial
55 dysfunction.

56 Tartary buckwheat (*Fagopyrum tataricum*) or common buckwheat is traditional crop
57 throughout the world, and has been used as an effective food in the treatment of CVD in the folk,
58 including diabetes, hypertension, hyperglycemia, hyperinsulinemia, and dyslipidemia.¹²⁻¹⁵
59 However, the specific components responsible for these effects and their mechanisms are still
60 not very clear. Interestingly, there is report showing that buckwheat contains multiple
61 flavonoids,¹⁶ and among them, rutin is shown to be the major buckwheat flavonoid responsible
62 for antioxidant, antiplatelet, anti-inflammatory, anti-hyperglycemic, antihypertensive, and
63 vasoprotective properties.¹⁷⁻²⁰ Besides, the vasoprotective effect of rutin was also involved in the
64 activation of endothelial nitric oxide (NO) synthetic system.²¹ Quercetin, as the aglycon of rutin,
65 is another important flavonoid in buckwheat that acts as a vasodilator in the vascular system.²²
66 Bhaskar et al. demonstrated that quercetin inhibited the formation of the plaques for its
67 antioxidant and anti-inflammatory effects in hypercholesterol diet-induced rabbits.²³ Recent
68 study also shows that intake of quercetin can increase NO production and improve endothelial
69 function, and lower cardiovascular risk due to its vasorelaxant and anti-oxidative properties.²⁴⁻²⁵
70 Interestingly, tartary buckwheat has recently received much attention as a natural flavonoid
71 source since it contains approximately 5-fold higher of rutin than common buckwheat.²⁶
72 However, the protective effects of flavonoids in tartary buckwheat on vascular dysfunction and
73 liver damage induced by consumption of a high TMAO diet have not yet been reported.

74 The present study was therefore designed to purify the flavonoid fraction (TBF) from Chinese
75 tartary buckwheat by AB-8 macroporous resin column, and its profile of compositional rutin and
76 quercetin was identified by HPLC. Furthermore, we also aimed to determine whether the
77 feeding of mice with 1.5% TMAO in tap water for 8 weeks caused the vascular and liver injury
78 in mice, and whether treatment with TBF attenuated TMAO-induced damage, and, if so,

79 whether the mechanisms underlying the process was involved the antioxidation and *e*NOS/NO
80 signaling. This paper provided a clue for substantiating dietary and therapeutic use of tartary
81 buckwheat in vascular dysfunction and hepatic injury.

82

83 **Materials and methods**

84 **Materials and Reagents**

85 The tartary buckwheat flour from whole seeds was obtained from Liangshan Qiongzhu Tartary
86 Buckwheat Products Co. Ltd. (Sichuan, China). AB-8 resin was purchased from Chemical Plant
87 of Nankai University (Tianjin, China). Chlorogenic acid, caffeic acid, rutin, hypericin, quercetin,
88 and phloretin were all obtained from the National Institute for the Control of Pharmaceutical and
89 Biological Products (Beijing, China). Trimethylamine-*N*-oxide (TMAO) was purchased from
90 Jinan Shangda Chemical Reagent Co. Ltd. (Jinan, China). Haematoxylin and eosin (H&E) and
91 oil red O were the products of Shanghai Lanji Technological Development Co. Ltd. (Shanghai,
92 China). Assay kits of serum total cholesterol (TC), total triglyceride (TG), high density
93 lipoprotein-cholesterol (HDL-C), low density lipoprotein-cholesterol (LDL-C), alanine
94 aminotransferase (ALT) and aspartate aminotransferase (AST) were purchased from Changchun
95 Huili Biotechnology Co., Ltd. (Changchun, China). Detection kits for nitric oxide (NO),
96 superoxide dismutase (SOD), glutathione peroxidase (GSH-Px), malonaldehyde (MDA) and
97 non-esterified fatty acid (NEFA) were the products of Nanjing Jiancheng Bioengineering
98 Institute (Nanjing, China). ELISA kits of endothelial nitric oxide synthase (*e*NOS), endothelin 1
99 (ET-1), prostaglandin I₂ (PGI₂), and thromboxane A₂ (TX-A₂) were also purchased from Nanjing
100 Jiancheng Bioengineering Institute (Nanjing, China). Deionized water was prepared using a
101 Millipore Milli Q-Plus system (Millipore, Bedford, MA, USA). Acetonitrile was purchased from
102 Acros-Organic (Geel, Belgium). All other reagents and chemicals were of analytical grade.

103 **Extraction of Tartary Buckwheat Flavonoids**

104 Flavonoid fraction of tartary buckwheat was isolated as previously described with some

105 modifications.²⁷ Approximately 2.5 kg of the dried tartary buckwheat flour was extracted by 25
106 L of methanol-water (75:25, v/v) with reflux for 2 h, and repeated three times. The combined
107 extracts were centrifuged at 3000g for 10 min, and concentrated at 60°C with a rotary
108 evaporator (RE-52AA, Shanghai, China) under vacuum, and then freeze-dried. The content of
109 rutin and quercetin in crude extract was 162.7 mg/g and 75.6 mg/g, respectively, which was
110 identified by HPLC, and deionized water was added to get rutin and quercetin solution at the
111 concentrations of 0.35 mg/mL and 0.16 mg/mL.

112 **Purification of Flavonoids Fraction from Tartary Buckwheat**

113 The purification of flavonoids-rich tartary buckwheat extract was performed as previously
114 described with some modifications.²⁸ The purification process was carried out on glass columns
115 (12 mm × 500 mm) wet-packed with 6 g (dry weight) AB-8 resin. Prior to the adsorption
116 experiment, the AB-8 resin was soaked in 95% ethanol, shaken for 24 h and subsequently
117 washed by deionized water thoroughly. The bed volume of resin was 30 mL. For the preliminary
118 test, 0.1 g of crude extract was mixed with 46.5 mL of deionized water (0.35 mg/mL of rutin and
119 0.16 mg/mL of quercetin), and then the sample solution was loaded on the glass column at a
120 flow rate of 1.5 mL/min. After adsorption, desorption was investigated by comparing the effect
121 of different concentrations of ethanol (40%, 50%, 60%, 70% and 80%) on desorption of
122 flavonoids at a flow rate of 1.5 mL/min, and fractions were collected and the concentrations of
123 rutin and quercetin were analyzed by HPLC. The enrichment of flavonoids was carried out in
124 the glass column with AB-8 resin under the optimized conditions. 160 mL of the sample solution
125 (0.35 mg/mL of rutin and 0.16 mg/mL of quercetin, pH 6.0) was applied to the glass column at
126 the flow rate of 1.5 mL/min. After reaching adsorptive saturation, the column was firstly washed
127 by deionized water to remove the soluble sugar and protein, and then eluted by ethanol-water
128 (pH 6.0) with a flow rate of 1.5 mL/min. The effluent liquid was collected until there was almost
129 no color, and then evaporated to dryness in a rotary evaporator at 60°C and freeze-dried. During
130 adsorption and desorption, aliquots were collected in 8 mL intervals by a Redifrac fraction

131 collector (BSZ-100, Shanghai, China). The purified tartary buckwheat flavonoid fraction was
132 named as TBF in this study, and this part was further applied in the following experiments for
133 the quantification of flavonoids and its protective effects on vascular endothelium and liver in
134 mice.

135 **HPLC Analysis for Flavonoid Profile in TBF**

136 The quantification of rutin and quercetin as major flavonoids in TBF was carried out using a
137 reversed-phase HPLC column (4.6 mm i.d. × 250 mm, 5 μm, Inertsil ODS-SP, Japan) on a
138 Shimadzu LC-2010 A HPLC system equipped with an UV detector, an autosampler and a
139 Shimadzu Class-VP 6.1 workstation software (SHIMADZU, Kyoto, Japan). The standards and
140 samples were all dissolved in 70% methanol aqueous solution to yield stock solution at the
141 concentration of 0.1 mg/mL. Before injection, all solutions were diluted and subsequently
142 filtered through a 0.45 μm Millipore membrane. A gradient elution was performed by varying
143 the proportion of solvent A (acetonitrile/water, 50:50, v/v) to solvent B (water containing 0.5%
144 formic acid). The gradient program was as follows: 0–30 min with 75% solvent B; 30–45 min
145 from 75% to 50% B; 45–55 min from 50% to 30% B, 55–60 min from 30% to 10% B, 60–65
146 min from 10% to 75% B. The flow rate of the mobile phase was 1 mL/min, and the UV
147 detection wavelength was 280 nm, and the sample injection volume was 25 μL at a 30°C
148 column temperature. The chromatographic peaks of the analytes were identified by comparison
149 of their retention time (t_R) values and UV spectra with those of known standards and determined
150 by peak areas from the chromatograms.

151 **Animals and Experimental Design**

152 Healthy male Kunming mice (weight 18-22 g) were purchased from the Experimental Animal
153 Center of Fourth Military Medical University (Xi'an, China). Mice were acclimatized for at least
154 7 days prior to use and were housed under standard conditions with 12/12 h light-dark cycle at
155 room temperature of $22 \pm 2^\circ\text{C}$ and humidity $60 \pm 5\%$. They were allowed free access to tap
156 water and rodent chow (40% corn flour, 26% wheat flour, 10% bran, 10% fish meal, 10% bean

157 cake, 2% mineral, 1% coarse, and 1% vitamin complex, Qianmin Feed Factory). All
158 experimental protocol used in this study was approved by the Committee on Care and Use of
159 Laboratory Animals of the Fourth Military Medical University, China (SYXK-007-2007). The
160 animals were randomly divided into five groups with 10 mice each: Normal control group,
161 high-TMAO control group (1.5% TMAO water alone), TBF-treated groups (200 mg/kg-bw for
162 low-dose group, 400 mg/kg-bw for middle-dose group, 800 mg/kg-bw for high-dose group,
163 supplemented with 1.5% TMAO water, respectively). The mice were allowed free access to tap
164 water or 1.5% TMAO water. The dosage of 1.5% TMAO was selected according to the previous
165 report,¹ and our pre-experimental results in mice. The capacity of water intake in mice was
166 monitored according to our previous experiments.²⁹ TBF was suspended in a 1% sodium
167 carboxymethylcellulose (CMC) aqueous solution and administered intragastrically (ig.) at 200,
168 400 and 800 mg/kg body weight once daily (0.4 mL) for 8 consecutive weeks, where the dosage
169 of TBF was optimized before the study in mice according to the results of our previous
170 experiments.³⁰ The mice from the normal and TMAO groups were also given the same volume
171 of vehicle, and 1.5% TMAO water was renewed every other day. The mouse body weight of all
172 the groups was measured once a week. Food and water intake was monitored daily, and then the
173 average food and water intake of each mouse in different groups was calculated. All the
174 administrations were conducted between eight and nine o'clock in the morning once daily. After
175 2 h, all of the animals were fasted but given enough water to drink for 12 h. At the end of the
176 experimental period, all of the animals were fully anesthetized by the inhalation of isoflurane,
177 and then the animals were sacrificed by cervical dislocation. Blood was withdrawn into a
178 syringe from the abdominal aorta, and mouse liver was immediately removed and washed by
179 ice-cold physiological saline.³¹ Blood samples were separated for serum aliquots by
180 centrifugation at 3000g for 10 min at 4 °C and stored at -20 °C for later biochemical analysis
181 within two weeks, while the isolated livers were refrigerated at -80°C. On the basis of the
182 records of the body weight and corresponding liver weight of every mouse, we calculated the

183 hepatosomatic index (HI) according to the following formula: $HI = \text{liver weight/body weight} \times$
184 100% . All the experiments were conducted according to the Guidelines of Experimental Animal
185 Administration published by the State Committee of Science and Technology of People's
186 Republic of China.

187 **Assay for Plasma NO and eNOS, and Serum ET-1, PGI₂, and TX-A₂ Levels**

188 Plasma NO levels were determined with a commercially available diagnostic kit, and the
189 results were expressed in $\mu\text{mol/L}$. Plasma eNOS and serum ET-1, PGI₂, and TX-A₂
190 concentrations were measured using competitive inhibition method of enzyme linked
191 immunosorbent ELISA assay kit according to the kit manufacturer's instructions, and the results
192 were expressed as units per litre (U/L), pg/mL, pg/mL, and pg/mL, respectively.

193 **Measurement of Serum Lipid Profile, and ALT and AST Activities**

194 The measurements for fasting serum TC, TG, LDL-C and HDL-C concentrations were
195 conducted by enzymatic colorimetric methods using commercial kits, and the results were all
196 expressed in mmol/L. The serum enzyme activities of ALT and AST were measured by
197 commercially available diagnostic kits. The enzymic activities were expressed as units per litre
198 (U/L).

199 **Assay of Hepatic NEFA, MDA, T-SOD and GSH-Px Levels**

200 The liver tissue was homogenized (10%, w/v) in ice-cold 50 mM phosphate buffer (pH 7.4)
201 by an automatic homogenate machine (F6/10-10G, FLUKO Equipment Shanghai Co. Ltd.,
202 Shanghai, China). During the preparation, 0.5 g of each hepatic tissue was homogenized in
203 9-fold frozen normal saline in volume, and centrifuged at 1500g for 10 min at 4°C. The
204 supernatant was collected for the measurements of NEFA, MDA, T-SOD and GSH-Px. The
205 protein concentration in homogenates was assayed by the method of Coomassie brilliant blue.³¹
206 The analysis for hepatic NEFA and MDA levels was performed with commercially available
207 diagnostic kits, and the results were expressed as $\mu\text{mol/g}$ protein and nmol/mg protein,
208 respectively. T-SOD and GSH-Px activities were assessed using common commercial kits, and

209 the results were expressed as U/mg protein.

210 **Histopathological Observation of Thoracic Aortas and Livers**

211 The thoracic aortas were stripped from any surrounding tissues and put in a buffer solution of
212 4% paraformaldehyde. Fixed tissues were processed routinely for paraffin embedding, and 5 μm
213 sections were prepared and dyed with hematoxylin and eosin (H&E). For H&E staining of the
214 liver, a portion of the liver from the left lobe was fixed in a 4% paraformaldehyde solution.
215 Fixed tissues were embedded in paraffin, cut into slices (5-6 μm thick), and stained with H&E
216 dye. For oil Red O staining, the liver sample was processed using cryostat (CM1950, Leika,
217 Germany) and then fixed and stained. The stained area was viewed using an optical microscope
218 at 400 \times . Finally, the images were examined and evaluated for pathological change analysis. The
219 cross-sectional areas of the intima, media, and lumen were calculated with a computerized
220 apparatus (VM-30, Olympus, Tokyo, Japan).

221 **Statistical Analysis**

222 All of the experiments were performed at least in triplicate. The data were expressed as means
223 of \pm SD (standard deviation), and subjected to an analysis of variance (ANOVA, $p < 0.05$) and
224 Duncan's multiple-range tests (SPSS, version 13.0). The p -value < 0.05 was considered
225 statistically significant.

226

227 **Results**

228 **Chemical Properties of TBF**

229 The extraction of crude flavonoids from the tartary buckwheat was performed with 75%
230 aqueous methanol. With this method, the extraction yield of crude extracts from tartary
231 buckwheat could reach approximately 9.2% (w/w) of the tartary buckwheat powder. The
232 purified tartary buckwheat flavonoids fraction (TBF) was further obtained from the crude
233 extracts by a separation on a AB-8 resin column. The effects of various concentrations of
234 aqueous ethanol as eluate on the recovery of rutin and quercetin were investigated. As a result,

235 60% aqueous ethanol was found to be the most effective for the recovery of rutin and quercetin
236 in the various elution systems. The yield of TBF was 1.8% (w/w) of the tartary buckwheat
237 powder.

238 A routine HPLC chromatographic procedure was performed to further measure the
239 component flavonoids in the flavonoid preparation. A HPLC chromatogram for single flavonoid
240 profile of TBF was illustrated in Fig. 1A, and the tested standard flavonoids were shown in Fig.
241 1B. The identification of component flavonoids was performed according to the retention time
242 (t_R) obtained from authentic standards under identical HPLC conditions. As depicted in Fig. 1B,
243 six peaks corresponding to authentic standards were identified in the order of chlorogenic acid
244 (12.1 min), caffeic acid (19.2 min), rutin (29.3 min), hypericin (30.5 min), quercetin (47.1 min),
245 and phloretin (53.5 min). In this study, linear regression was assessed for the content calculation,
246 and the assay had excellent linearity between Y (peak area of analyte) and X (concentration of
247 analyte). The regression lines for rutin and quercetin were $Y = 1.1E+5X + 8460.2$ ($R^2 = 0.9999$,
248 $n = 5$), and $Y = 1864.2X + 35712$ ($R^2 = 0.9993$, $n = 5$), respectively. As shown in Fig. 1A, HPLC
249 analysis clearly indicated that the major flavonoids present in purified TBF were rutin and
250 quercetin, and their contents were 536.2 mg/g and 371.6 mg/g, respectively, accounting for up to
251 90.8% of TBF, suggesting that TBF is a flavonoid fraction with high-purity.

252 **Effects of TBF on body weight, liver weight, and liver index in mice**

253 As can be seen in Table 2, after giving 1.5% TMAO for 8 weeks, the average food and water
254 intake was not significantly different among all the tested groups, where the daily food intake
255 was between 9.77 ± 1.68 g/mice/day and 10.29 ± 2.11 g/mice/day, and water consumption was
256 between 6.32 ± 3.25 mL/mice/day and 6.53 ± 2.16 mL/mice/day. However, the mice fed a high
257 TMAO diet significantly increased the body weight, liver weight and HI from 46.28 ± 2.76 g,
258 2.04 ± 0.11 g, and 4.41 ± 0.28 g in normal group to 48.97 ± 2.03 g ($p < 0.05$), 2.44 ± 0.15 g ($p <$
259 0.01), and 4.97 ± 0.33 g ($p < 0.01$), respectively. Interestingly, the increased liver weight could
260 be well decreased by the oral administration of middle- and high- doses of TBF ($p < 0.01$).

261 Additionally, treatment with TBF at 400 and 800 mg/kg·bw also significantly attenuated the
262 increases in body weight ($p < 0.05$) and dose-dependently decreased the HI ($p < 0.05$, $p < 0.01$)
263 of TMAO-treated mice. However, supplementation with TBF at a low dose led to the slight
264 decreases in body weight, liver weight and HI, but there was no statistical significance ($p >$
265 0.05). The present result suggests that TBF can inhibit the TMAO-induced weight gain.

266 **Effects of TBF on Plasma NO and eNOS, and Serum ET-1 Levels in Mice**

267 Endothelium plays an important role in the regulation of vascular tone, and an imbalance
268 between vasodilator NO and vasoconstrictor endothelin-1 (ET-1) causes endothelial
269 dysfunction.³²⁻³³ As can be seen in Fig. 2A and B, after giving 1.5% high-TMAO water for 8
270 weeks, plasma NO level and eNOS activity in TMAO-fed mice sharply decreased to 3.9 ± 0.7
271 $\mu\text{mol/L}$ ($p < 0.01$) and 12.5 ± 3.3 U/L ($p < 0.01$) from 5.3 ± 0.5 $\mu\text{mol/L}$ and 26.5 ± 6.1 U/L of the
272 untreated normal mice, respectively, suggesting that TMAO caused vascular endothelial injury
273 in mice. Interestingly, the tested mice receiving oral administration of TBF at 200, 400 and 800
274 mg/kg·bw had an increase by 7.9% ($p > 0.05$), 27.3% ($p < 0.05$) and 42.3% ($p < 0.01$) in plasma NO
275 levels, relative to TMAO-treated mice, respectively (Fig. 2A). Similarly, plasma eNOS activity
276 was also increased by 17.5% ($p > 0.05$), 55.4% ($p < 0.01$) and 99.1% ($p < 0.01$) following the
277 treatment, respectively (Fig. 2B), indicating the protective effect of TBF on TMAO-induced
278 endothelial injury in mice. As shown in Fig. 2C, application of high TMAO-fed diet in mice
279 caused a severe increase in serum ET-1 concentrations from 64.3 ± 9.5 pg/mL of the normal
280 mice to 91.6 ± 10.1 pg/mL ($p < 0.01$), suggesting that 1.5% TMAO feeding might cause
281 endothelial injury in mice. However, this TMAO-induced increase was effectively attenuated by
282 the supplementation of medium-dose or high-dose of TBF with a 38.3% or 50.3% decrease,
283 relative to TMAO-fed mice, respectively ($p < 0.01$). However, the co-treatment with TBF at a low
284 dose of 200 mg/kg·bw led to a slight decrease in the level of serum ET-1, but there was no
285 statistical significance ($p > 0.05$). The present results suggest that TBF can significantly inhibit
286 the TMAO-induced endothelial injury in mice.

287 **Effects of TBF on Serum PGI₂ and TX-A₂ Levels in Mice**

288 PGI₂ and TX-A₂ are the most common prostanoids in the cardiovascular system, which act as
289 opposite roles in the formation of atherosclerosis.³⁴ Herein, we further examined the serum PGI₂
290 and TX-A₂ concentrations in the mice exposed to high TMAO diet in the water. As expected, the
291 mice exposed to 1.5% TMAO water had a 40.3% decrease in serum PGI₂ concentration, and a
292 24.2% increase in serum TX-A₂ level, respectively ($p<0.01$, Fig. 2D and E). However, the low
293 PGI₂ and high TX-A₂ levels in TMAO-fed mice could be prevented by TBF administration in a
294 dose-dependent manner, especially when the dosage increased to 400 and 800 mg/kg·bw. As
295 depicted in Fig. 2D and E, serum PGI₂ levels of the mice treated with TBF at 400 and 800
296 mg/kg·bw were significantly increased by 42.9% ($p<0.05$) and 95.2% ($p<0.01$), as compared to
297 TMAO-fed mice, respectively, and serum TX-A₂ levels of the mice treated with middle- and
298 high-doses of TBF were remarkably lowered by 29.2% and 49.6%, ($p<0.01$ vs TMAO alone
299 group), respectively. However, administration of TBF at a low dose of 200 mg/kg·bw led to a
300 slight increase in the serum PGI₂ and a slight decrease in the serum TX-A₂, but there was no
301 statistical significance ($p>0.05$).

302 **Effects of TBF on Serum Lipid Profiles in Mice**

303 Excess LDL and TG together with HDL are well known to be targets of therapy during
304 management of CVD.³⁵ Herein, we further examined the serum lipid profiles in mice fed high
305 TMAO diet that contributed to the CVD risk. As shown in Table 1, the levels of serum TC, TG,
306 and LDL-C were elevated dramatically and HDL-C had an expected decline in the high
307 TMAO-fed mice, where the levels of TC, TG and LDL-C had a significant increase by 34.6%
308 ($p<0.01$), 86.6% ($p<0.01$) and 35.2% ($p<0.01$), and HDL-C had a remarkable decrease by 29.8%
309 ($p<0.01$), relative to the untreated mice, respectively, indicating that high TMAO diet caused the
310 hyperlipidemia in mice. However, the protective administration of TBF could effectively
311 decrease the serum TC, TG and LDL-C levels and increase the HDL-C concentration. It was
312 also noted that the levels of TC, TG, LDL-C and HDL-C of high doses of TBF-treated mice

313 were close to that of the normal mice, suggesting that TBF might normalize the dyslipidemia by
314 improving the serum lipid profiles in high TMAO-induced mice.

315 **Aortic Pathology and Protective Effects of TBF**

316 Histopathological observation of the aorta was performed to further support the evidence for
317 the biochemical analysis. As shown in Fig. 3A, the histology of the aortas appeared normal in
318 the untreated normal mice, while the endothelium of the aorta wall of TMAO-induced mice
319 showed extensive vascular injuries, characterized by significant proliferation of the wall,
320 irregular medium and internal elastic lamina in the wall. Interestingly, the administration of TBF
321 protected the vascular endothelium from damage of high TMAO, where the structures of the
322 arteries had a significant reduction of aorta thickness in a dose-dependent manner, when
323 compared with TMAO-fed mice. The administration of TMAO along with TBF at 800
324 mg/kg·bw showed near normal appearance, suggesting that TBF could protect the blood vessel
325 from TMAO-induced damage.

326 In addition, the results of intima/media ratio further confirmed that TBF effectively stabilized
327 the vessels against TMAO as seen by the reduction of wall thickness ratio (Fig. 3B). As depicted
328 in Fig. 3B, the TMAO-fed mice had a 0.5-fold increase in intima/media ratio, compared to the
329 untreated normal mice ($p<0.01$). However, the intima/media ratios of the mice treated with 200,
330 400 and 800 mg/kg·bw TBF was lowered by 13.3% ($p>0.05$), 26.7% ($p<0.05$) and 40.1%
331 ($p<0.01$), respectively, relative to TMAO-treated mice. These results together with biochemical
332 marks demonstrate that TBF can protect vascular tissue from TMAO-induced vessel injury and
333 vascular dysfunction.

334 **Effects of TBF on Serum ALT and AST Levels in Mice**

335 To further test whether TMAO as oxidant would cause oxidative damage of the liver, the
336 activities of serum ALT and AST, an indicator of leakage of hepatocytes into circulation under
337 hepatotoxicity,³⁶ were evaluated in TMAO-treated mice. As shown in Fig. 4A and B, the
338 enzymatic activities of serum ALT and AST in TMAO-treated mice were remarkably increased

339 to 103.2 ± 15.0 U/L ($p < 0.01$) and 180.2 ± 26.2 U/L ($p < 0.01$) from 75.0 ± 12.9 U/L and $135.4 \pm$
340 14.3 U/L of the normal mice, respectively, indicating that the intake of high TMAO diet caused
341 the hepatotoxicity in mice. However, the protective administration of TBF with a supplement of
342 1.5% TMAO water decreased the activities of these functional markers, relative to
343 TMAO-treated mice. As illustrated Fig. 4A, the co-treatment of TBF at 400 and 800 mg/kg·bw
344 once daily for 8 consecutive weeks dose-dependently reduced the TMAO-induced elevation of
345 serum ALT activity ($p < 0.05$, $p < 0.01$). Meanwhile, administration of TBF at 400 and 800
346 mg/kg·bw significantly lowered the AST activities by 31.77% and 39.83% ($p < 0.01$, Fig. 4B),
347 as compared to HF-fed mice, respectively, suggesting that TBF exhibited strong protective
348 effects against TMAO-induced liver injury in mice.

349 **Effects of TBF on Hepatic NEFA, MDA, T-SOD and GSH-Px Levels**

350 As shown in Fig. 5A, hepatic NEFA levels in TMAO-fed mice were significantly increased as
351 compared to the normal mice from 51.7 ± 17.1 $\mu\text{mol/gprot}$ to 116.4 ± 16.5 $\mu\text{mol/gprot}$ ($p < 0.01$).
352 As expected, hepatic NEFA contents were significantly lowered by 21.0% ($p < 0.01$), 34.9%
353 ($p < 0.01$) and 52.4% ($p < 0.01$) in the mice treated with TBF at 200, 400, and 800 mg/kg·bw,
354 when compared to TMAO-fed mice, respectively. In addition, the hepatic MDA, a hallmark of
355 oxidative modification to membrane lipids in liver,³⁷ was significantly increased from 2.8 ± 1.0
356 nmol/mgprot of normal group to 6.3 ± 0.6 nmol/mgprot ($p < 0.01$) in the mice fed 1.5% TMAO
357 for 8 weeks (Fig. 5B), indicating that high TMAO diet caused notable liver peroxidation damage
358 in mice. However, this TMAO-induced increase was effectively attenuated by the co-treatment
359 with TBF at the tested dosages of 400 and 800 mg/kg·bw, respectively ($p < 0.01$), but no
360 significant decrease in MDA level was observed in the mice treated with 200 mg/kg·bw of TBF
361 ($p > 0.05$). Furthermore, continuous feeding of TMAO in mice caused characteristic
362 hepatotoxicity in antioxidant parameters of liver tissue, as reflected by 31.4% decrease of
363 hepatic T-SOD activity ($p < 0.01$) and 29.5% decrease of hepatic GSH-Px activity ($p < 0.01$) in
364 TMAO-treated mice (Fig. 5C and D). However, TMAO-induced inhibition in antioxidant

365 enzyme activities was obviously prevented by the supplementation with TBF at 400 ($p<0.05$)
366 and 800 mg/kg·bw ($p<0.01$), and this protection effect could be performed in a dose-dependent
367 manner.

368 **Histopathological Examination of Mouse Liver**

369 Histopathological observations of H&E (Fig. 6) and oil red O staining (Fig. 7) of the livers
370 were investigated to further support the protective effect of TBF against TMAO-induced
371 hepatocyte morphological changes. In the normal group, liver slices showed typical hepatic cells
372 with well-preserved cytoplasm, prominent nucleus and nucleolus, and visible central veins (Fig.
373 6A). In TMAO-fed mice, the liver sections showed a parenchymal disarrangement, such as
374 hepatocyte necrosis, cytoplasmic vacuolation, and the loss of cellular boundaries (Fig. 6B).
375 However, the hepatic lesions caused by TMAO were markedly ameliorated by the co-treatment
376 with TBF, and TBF at 400 and 800 mg/kg·bw was more effective when compared with 200
377 mg/kg·bw, showing near normal appearance with well-preserved cytoplasm, prominent nuclei,
378 and legible nucleoli, and this protective effect was dose-dependent (Fig. 6C-E). In addition, the
379 photomicrographs of oil red O staining of the liver specimens were investigated, and compared
380 with the normal mice (Fig. 7A). As shown in Fig. 7B, the liver of TMAO-fed mice showed
381 widespread deposition of lipid droplets inside the parenchyma cells. However, the mice treated
382 with TBF showed scattered droplets of fat when compared with high TMAO-fed mice, and
383 especially, TBF at 800 mg/kg·bw showed near normal appearance as comparable to the normal
384 mice (Fig. 7C-E). These results together with biochemical analysis demonstrated that TBF could
385 protect liver tissue from high TMAO-induced fatty liver and hepatic damage in mice.

386

387 **Discussion**

388 It is recently known that high ingestion of trimethylamine-containing nutrients, such as
389 choline, *L*-carnitine, lecithin and their metabolite TMAO, is linked to atherosclerosis.^{1,3} Recently,
390 tartary buckwheat has been reported to have potential effects in the prevention of CVD.¹³⁻¹⁴

391 Rutin and quercetin are the main bioactive constituents presented in tartary buckwheat, and play
392 important role in improving endothelial function and attenuating atherosclerosis.^{19,24} However,
393 there are no reports in linking the protective effects of flavonoids derived from tartary
394 buckwheat to the endothelial dysfunction and liver injury caused by TMAO. In the present study,
395 the mice fed with 1.5% high TMAO water for continuous 8 weeks was shown to have
396 significant vascular injury, which was consistent with recent findings.^{1,3} Besides, our study also
397 firstly found that high TMAO supplementation of mice caused severe liver injury via oxidative
398 damage and lipid peroxidation. Furthermore, it was of interest that the purified tartary
399 buckwheat flavonoids (TBF) were firstly demonstrated to exhibit vasoprotective and
400 hepatoprotective effects against dietary TMAO-induced liver and vascular damage in mice.

401 NO is produced by *e*NOS, and plays an important role in regulating the diameter of blood
402 vessels and maintaining an anti-proliferative and anti-inflammatory environment in the vessel
403 wall.³⁸⁻³⁹ Endothelial dysfunction is thought to arise due to a reduction in the
404 bioavailability/bioactivity of NO, and the *e*NOS dysfunctions can accelerate atherosclerosis.³² In
405 our study, supplementation of 1.5% high TMAO water markedly decreased the serum NO and
406 *e*NOS levels ($p<0.01$) in mice. However, the mice administrated with TBF at 400 and 800
407 mg/kg-bw for 8 consecutive weeks remarkably elevated the TMAO-lowered NO and *e*NOS
408 levels, respectively, implying that TBF might effectively prevent endothelial dysfunction by
409 stimulating synthesis of NO. ET-1 is another regulator of vascular tone and an increase in
410 circulating ET-1 levels indicates the dysfunction of vascular endothelium.⁴⁰ Consistent with this
411 finding, application of 1.5% high TMAO water in mice also showed a striking increase in ET-1
412 levels, as compared to the untreated normal mice ($p<0.01$), and TBF was shown to significantly
413 block the increase of serum ET-1 in mice (Fig. 2C). It is well known that NO is a feed-back
414 inhibitor of ET-1 release, and an increase in NO excretion also leads to the decrease in ET-1
415 levels.⁴¹ The results presented here indicate that TBF exhibits effective protection of vascular
416 cells by up-regulation of NO and inhibition of ET-1 release, thus helping to maintain the balance

417 between these two vasoactive components. This result agrees with the previous studies showing
418 that rutin exerts endothelium-dependent vasorelaxation action by mediating NO/cGMP
419 pathways,⁴² and quercetin administration reduces arterial pressure in hypertensive men by
420 lowering the ratio of circulating ET-1 to NO, and this alteration will improve endothelial
421 function.⁴³

422 PGI₂ and TX-A₂, a pair of common prostanoids, play an opposite role in regulation of
423 cardiovascular homeostasis, which are associated with endothelial dysfunction and are an early
424 marker of atherosclerosis.³⁴ PGI₂ induces vascular relaxation and potently inhibits platelet
425 activation, and exerts the protective effect on cardiovascular system, whereas TX-A₂ is a potent
426 vasoconstrictor and a strong platelet activator, which works as a factor facilitating the
427 development of atherosclerosis.^{34,44} In our study, TBF could significantly dispute the decrease of
428 serum PGI₂ concentration and the increase of serum TX-A₂ level caused by high TMAO feeding
429 (Fig. 2), suggesting that TBF prevented the vascular endothelial impairments induced by TMAO
430 by modulating the balance between serum PGI₂ and TX-A₂. In addition, histopathological
431 examination also showed that the TMAO-induced pathological damage of mouse aortic vessel
432 was markedly reduced by the administration of TBF (Fig. 3A), as reflected by the reduced
433 thickness of the tunica intima of the aorta, relative to TMAO-treated mice (Fig. 3B). This
434 finding obviously demonstrated that TBF produced a protective effect on aortic pathology in the
435 mice fed with high TMAO diet, and the protective effect was consistent with some previous
436 studies, where rutin increased capillary fragility and decreased the permeability of the vessels,
437 and quercetin restored the impaired endothelial function in several animal models.^{16,45}

438 It is widely recognized that abnormal lipid metabolism is an early indication of CVD, and
439 lipids play a key part in the pathogenesis of plaques.³⁵ In our study, high-TMAO feeding caused
440 obvious dyslipidaemia in the experimental mice, reflected by elevated levels of TC, TG, and
441 LDL-C, and lowered levels of HDL-C (Table 1). The results implied that the intake of high
442 TMAO disordered lipid mechanism of liver that might promote lipid deposition in hepatocytes

443 and adipocytes, resulting in hyperlipidemia or fatty liver. However, co-treatment of TBF had an
444 efficient enhance in HDL-C levels and a significant decrease in TC, TG and LDL-C levels
445 against high TMAO diet in mice. It was also observed that the high TMAO diet induced the
446 weight gain of the body and liver, and hepatosomatic index, and this effect was prevented by
447 TBF treatment (Table 2). The result was consistent with the previous studies showing that both
448 rutin and quercetin could suppress body weight gain and improve lipid profile in serum or liver,
449 indicating that TBF might interfere with lipid mechanism and decrease the lipid synthesis in
450 mice.^{46,47} The oil-red-O staining result of liver tissues further confirmed that TBF could
451 normalize the dyslipidemia induced by TMAO diet and protected the liver from chronic dietary
452 TMAO-induced histopathological alteration (Fig. 7C-E), suggesting that TBF could play a
453 protective role against hyperlipidemia in high TMAO-fed mice.

454 Nevertheless, considering the typical oxidation property of TMAO, we further assessed the
455 oxidative damage of livers in the mice fed with TMAO. As shown in Fig. 4, application of high
456 TMAO diet markedly raised serum AST and ALT activities in mice, uniquely indicating that the
457 livers in TMAO-fed mice were damaged because the increased ALT activity was an indicator of
458 cell membrane damage, and the elevated AST activity is another indicator of mitochondrial
459 damage.⁴⁸ However, it was noted that the alterations of AST and ALT activities were observably
460 mitigated by the co-treatment of TBF, suggesting that TBF not only stabilized the hepatic
461 cellular membrane, but also had a protective effect on mitochondria.⁴⁸

462 As reported, high NEFA level can lead to hepatic mitochondrial swelling, and permeability
463 increasing, as well as lipid peroxidation,⁴⁹ and MDA is the final stage of lipid peroxidation of
464 the polyunsaturated fatty acid of biological membrane,⁵⁰ which can result in failure of the
465 antioxidant defense mechanisms to prevent the formation of excessive reactive oxygen species
466 (ROS).³² In our study, intake of 1.5% TMAO diet caused a significant increase in hepatic NEFA
467 and MDA contents of the mice, as compared to the normal group, respectively ($p < 0.01$, Fig. 5A
468 and B). However, protective administration of TBF significantly reduced the hepatic NEFA and

469 MDA levels against oxidative stress induced by TMAO. These results indicate that TBF can
470 effectively scavenge the non-esterified fatty acid released in the liver and successfully block the
471 oxidative chain reaction, and this may be related to the high radical scavenging activity of rutin
472 and quercetin.²⁶

473 SOD and GSH-Px are the major natural antioxidant enzymes which play important roles in
474 the elimination of ROS derived from the redox process in liver tissues.⁵⁰ For example, SOD
475 catalyzes the dismutation of superoxide anions into hydrogen peroxide that subsequently
476 converts to water by GSH-Px or converts lipid hydroperoxides to nontoxic alcohols.³¹ Here,
477 mice treated with TMAO water showed a sharp decrease in antioxidant capacity of the liver as
478 evidenced by inhibiting the enzymic activities of SOD and GSH-Px ($p < 0.01$, Fig. 5C and D).
479 Interestingly, the inhibitory enzymes were significantly increased by co-treatment with TBF at
480 400 or 800 mg/kg·bw, suggesting that it could protect the antioxidant enzymes or activate the
481 enzyme activity in TMAO-damaged liver tissue, and these protective effects might be due to the
482 strong antioxidant capacity of rutin and quercetin.^{14,17} In further histopathological examination,
483 the mice fed with 1.5% high TMAO water showed distinct necrosis, ballooning degeneration,
484 and inflammatory cell infiltration of the liver, which might be due to prevention of the toxic
485 chemical reactions from the formation of highly ROS induced by TMAO. However, the
486 co-treatment with TBF, especially at dosage of 800 mg/kg·bw (Fig. 6E), showed nearly normal
487 cellular architecture with distinct hepatic cells, suggesting that these histological alterations
488 were observably attenuated by TBF. Taken together, this was the first investigation with
489 unequivocal evidence that TBF could inhibit TMAO-induced hepatic oxidative injury in mice.

490 In conclusion, data presented in this study for the first time demonstrated that dietary intake
491 of high TMAO was highly associated with liver oxidative damage, and tartary buckwheat
492 flavonoids as TBF exerted systematic protective effect against TMAO-induced endothelial
493 dysfunction and hepatotoxicity in mice through inhibiting TMAO-induced ROS generation and
494 increasing vascular NO production. The present study may provide important evidences in

495 finding novel TMAO-based nutritional target for intervention in vascular dysfunction and liver
496 diseases in humans. Results of our study also indicate that TBF may play an important role in
497 interfering TMAO-mediated damage mechanism of high methyl-donor diet-caused endothelial
498 dysfunction and liver diseases.

499

500 **Acknowledgements**

501 This study was supported by the grants from the National Natural Science Foundation of
502 China (C31171678), and the Fundamental Research Funds for the Central Universities of
503 Shaanxi Normal University, China (GK201103004).

504

505 **References**

- 506 1 Z. N. Wang, E. Klipfell, B. J. Bennett, R. Koeth, B. S. Levison, B. DuGar, A. E. Feldstein, E.
507 B. Britt, X. M. Fu, Y. M. Chung, Y. P. Wu, P. Schauer, J. D. Smith, H. Allayee, W. H. W.
508 Tang, J. A. DiDonato, A. J. Lusis, S. L. Hazen, Gut flora metabolism of
509 phosphatidyl-choline promotes cardiovascular disease, *Nature*, 2011, **472**, 57-63.
- 510 2 J. Y. Zhang, R. X. Liang, L. Wang, R. Y. Yan, R. Hou, S. R. Gao, B. Yang, Effects of an
511 aqueous extract of *Crataegus pinnatifida* Bge. var. *major* N.E.Br. fruit on experimental
512 atherosclerosis in rats, *J. Ethnopharmacol.*, 2013, **148**, 563-569.
- 513 3 R. A. Koeth, Z. Wang, B. S. Levison, J. A. Buffa, E. Org, B. T. Sheehy, E. B. Britt, X. Fu, Y.
514 Wu, L. Li, J. D. Smith, J. A. DiDonato, J. Chen, H. Li, G. D. Wu, J. D. Lewis, M. Warriar,
515 J. M. Brown, R. M. Krauss, W. H. W. Tang, F. D. Bushman, A. J. Lusis, S. L. Hazen,
516 Intestinal microbiota metabolism of *L*-carnitine, a nutrient in red meat, promotes
517 atherosclerosis, *Nature Med.*, 2013, **19**, 576-585.
- 518 4 W. H. W. Tang, Z. Wang, B. S. Levison, R. A. Koeth, E. B. Britt, X. Fu, Y. Wu, S. L. Hazen,
519 Intestinal microbial metabolism of phosphatidylcholine and cardiovascular risk, *N. Engl. J.*

- 520 *Med.*, 2013, **368**, 1575-1584.
- 521 5 B. J. Bennett, T. Q. De Aguiar Vallim, Z. N. Wang, D. M. Shih, Y. H. Meng, J. Gregory, H.
522 Allayee, R. Lee, M. Graham, R. Crooke, P. A. Edwards, S. L. Hazen, A. J. Lusis,
523 Trimethylamine-*N*-Oxide, a metabolite associated with atherosclerosis, exhibits complex
524 genetic and dietary regulation, *Cell Metab.*, 2013, **17**, 49-60.
- 525 6 M. Candiracci, B. Citterio, E. Piatti, Antifungal activity of the honey flavonoid extract against
526 *Candida albicans*, *Food Chem.*, 2012, **131**, 493-499.
- 527 7 K. N. C. Murthy, J. Kim, A. Vikram, B. S. Patil, Differential inhibition of human colon cancer
528 cells by structurally similar flavonoids of citrus, *Food Chem.*, 2012, **132**, 27-34.
- 529 8 K. Mkyneen, S. Jitsaardkul, P. Tachasamran, N. Sakai, S. Puranachoti, N. Nirojsinlapachai, V.
530 Chattapat, N. Caengprasath, S. Ngamukote, S. Adisakwattana, Cultivar variations in
531 antioxidant and antihyperlipidemic properties of pomelo pulp (*Citrus grandis* [L.] Osbeck)
532 in Thailand, *Food Chem.*, 2013, **139**, 735-743.
- 533 9 C. D. Kay, L. Hooper, P. A. Kroon, E. B. Rimm, A. Cassidy, Relative impact of flavonoid
534 composition, dose and structure on vascular function: A systematic review of randomised
535 controlled trials of flavonoid-rich food products, *Mol. Nutr. Food Res.*, 2012, **56**,
536 1605-1616.
- 537 10 A. Scalbert, C. Manach, C. Morand, C. Remesy, L. Jimenez, Dietary polyphenols and the
538 prevention of diseases, *Crit. Rev. Food Sci.*, 2005, **45**, 287-306.
- 539 11 E. Middleton, C. Kandaswami, T. C. Theoharides, The effects of plant flavonoids on
540 mammalian cells: implications for inflammation, heart disease, and cancer, *Pharmacol.*
541 *Rev.*, 2000, **52**, 673-751.
- 542 12 L. Costantini, L. Lukšič, R. Molinari, I. Kreft, G. Bonafaccia, L. Manzi, L. Merendino,
543 Development of gluten-free bread using tartary buckwheat and chia flour rich in flavonoids
544 and omega-3 fatty acids as ingredients, *Food Chem.*, 2014, **165**, 232-240.
- 545 13 H. Kim, K. J. Park, J. H. Lim, Metabolomic analysis of phenolic compounds in buckwheat

- 546 (*Fagopyrum esculentum* M.) sprouts treated with methyl jasmonate, *J. Agric. Food Chem.*,
547 2011, **59**, 5707-5713.
- 548 14 D. Li, X. L. Li, X. L. Ding, Composition and antioxidative properties of the flavonoid-rich
549 fractions from tartary buckwheat grains, *Food Sci. Biotechnol.*, 2010, **19**, 711-716.
- 550 15 K. Nakamura, K. Naramoto, M. Koyama, Blood-pressure-lowering effect of fermented
551 buckwheat sprouts in spontaneously hypertensive rats, *J. Funct. Foods*, 2013, **5**, 406-415.
- 552 16 N. Fabjan, J. Rode, I. J. Kosir, Z. Wang, Z. Zhang, I. Kre, Tartary buckwheat (*Fagopyrum*
553 *tataricum* Gaertn.) as a source of dietary rutin and quercitrin, *J. Agric. Food Chem.*, 2003,
554 **51**, 6452-6455.
- 555 17 S. J. Hur, S. J. Park, C. H. Jeong, Effect of buckwheat extract on the antioxidant activity of
556 lipid in mouse brain and its structural change during *in vitro* human digestion, *J. Agric.*
557 *Food Chem.*, 2011, **59**, 10699-10704.
- 558 18 P. Jiang, F. Burczynski, C. CamTFell, G. Pierce, J. A. Austria, C. J. Briggs, Rutin and
559 flavonoid contents in three buckwheat species *Fagopyrum esculentum*, *F. tataricum*, and *F.*
560 *homotropicum* and their protective effects against lipid peroxidation, *Food Res. Int.*, 2007,
561 **40**, 356-364.
- 562 19 J. R. Sheu, G. Hsiao, P. H. Chou, M. Y. Shen, D. S. Chou, Mechanisms involved in the
563 antiplatelet activity of rutin, a glycoside of the flavonol quercetin, in human platelets, *J.*
564 *Agric. Food Chem.*, 2004, **52**, 4414-4418.
- 565 20 F. Mellou, H. Loutrari, H. Stamatis, C. Roussos, F. N. Kolisis, Enzymatic esterification of
566 flavonoids with unsaturated fatty acids: effect of the novel esters on vascular endothelial
567 growth factor release from K562 cells, *Process Biochem.*, 2006, **41**, 2029-2034.
- 568 21 F. Fusi, S. Saponara, F. Pessina, B. Gorelli, G. Sgaragli, Effects of quercetin and rutin on
569 vascular preparations, *Eur. J. Nutr.*, 2003, **42**, 10-17.
- 570 22 J. V. Formica, W. Regelson, Review of the biology of quercetin and related bioflavonoids,
571 *Food Chem. Toxicol.*, 1995, **33**, 1061-1080.

- 572 23 S. Bhaskar, K. S. Kumar, K. Krishnan, H. Antony, Quercetin alleviates hypercholesterolemic
573 diet induced inflammation during progression and regression of atherosclerosis in rabbits,
574 *Nutrition*, 2013, **29**, 219-229.
- 575 24 N. K. H. Khoo, C. R. White, L. Pozzo-Miller, F. Zhou, C. Constance, T. Inoue, R. P. Patel, D.
576 A. Parks, Dietary flavonoid quercetin stimulates vasorelaxation in aortic vessels, *Free*
577 *Radic. Biol. Med.*, 2010, **49**, 339-347.
- 578 25 J. M. Hodgson, K. D. Croft, Dietary flavonoids: effects on endothelial function and blood
579 pressure, *J. Sci. Food Agric.*, 2006, **86**, 2492-2498.
- 580 26 C. L. Liu, Y. S. Chen, J. H. Yang, B. H. Chiang, Antioxidant activity of tartary (*Fagopyrum*
581 *tataricum* (L.) Gaertn.) and common (*Fagopyrum esculentum* Moench) buckwheat sprouts,
582 *J. Agric. Food Chem.*, 2008, **56**, 173-178.
- 583 27 C. C. Lee, S. R. Shen, Y. J. Lai, S. C. Wu, Rutin and quercetin, bioactive compounds from
584 tartary buckwheat, prevent liver inflammatory injury, *Food Funct.*, 2013, **4**, 794-802.
- 585 28 Z. Y. Zhao, L. L. Dong, Y. L. Wu, F. Lin, Preliminary separation and purification of rutin and
586 quercetin from *Euonymus alatus* (Thunb.) Siebold extracts by macroporous resins, *Food*
587 *Bioprod. Process*, 2011, **89**, 266-272.
- 588 29 Y. Zhao, X. B. Yang, D. Y. Ren, D. Y. Wang, Y. Xuan, Preventive effects of jujube
589 polysaccharides on fructose-induced insulin resistance and dyslipidemia in mice, *Food*
590 *Funct.*, 2014, **5**, 1771-1778.
- 591 30 Y. M. Cui, X. B. Yang, X. S. Lu, J. W. Chen, Y. Zhao, Protective effects of
592 polyphenols-enriched extract from Huangshan Maofeng green tea against CCl₄-induced
593 liver injury in mice, *Chem-Biol. Interact.*, 2014, **220**, 75-83.
- 594 31 R. J. Zhang, Y. Zhao, Y. F. Sun, X. S. Lu, X. B. Yang, Isolation, characterization, and
595 hepatoprotective effects of the raffinose family oligosaccharides from *Rehmannia glutinosa*
596 Libosch, *J. Agric. Food Chem.*, 2013, **61**, 4857786-4857793.
- 597 32 S. R. Thomas, P. K. Witting, G. R. Drummond, Redox control of endothelial function and

- 598 dysfunction: molecular mechanisms and therapeutic opportunities, *Antioxid. Redox Signal.*,
599 2008, **10**, 1713-1765.
- 600 33 D. E. Kohan, N. F. Rossi, E. W. Inscho, D. M. Pollock, Regulation of blood pressure and salt
601 homeostasis by endothelin, *Physiol. Rev.*, 2011, **91**, 71-77.
- 602 34 K. Yuhki, F. Kojima, H. Kashiwagi, J. Kawabe, T. Fujino, S. Narumiya, F. Ushikubi, Roles of
603 prostanoids in the pathogenesis of cardiovascular diseases: Novel insights from knockout
604 mouse studies, *Pharmacol. Ther.*, 2011, **129**, 195-205.
- 605 35 M. U. Imam, A. Ishaka, D. Ooi, N. D. M. Zamri, N. Sarega, M. Ismail, N. M. Esa,
606 Germinated brown rice regulates hepatic cholesterol metabolism and cardiovascular disease
607 risk in hypercholesterolaemic rats, *J. Funct. Foods*, 2014, **8**, 193-203.
- 608 36 C. C. Huang, Y. T. Tung, K. C. Cheng, J. H. Wu, Phytocompounds from *Vitis kelungensis*
609 stem prevent carbon tetrachloride-induced acute liver injury in mice, *Food Chem.*, 2011,
610 **125**, 726-731.
- 611 37 Y. F. Sun, X. B. Yang, X. S. Lu, D. Y. Wang, Y. Zhao, Protective effects of Keemun black tea
612 polysaccharides on acute carbon tetrachloride-caused oxidative hepatotoxicity in mice,
613 *Food Chem. Toxicol.*, 2013, **58**, 184-192.
- 614 38 S. Dimmeler, I. Fleming, B. Fisslthaler, C. Hermann, R. Busse, A. M. Zeiher, Activation of
615 nitric oxide synthase in endothelial cells by Akt-dependent phosphorylation, *Nature*, 1999,
616 **399**, 601-605.
- 617 39 W. C. Sessa, eNOS at a glance, *J. Cell Sci.*, 2004, **117**, 2427-2429.
- 618 40 M. Gómez-Guzmán, R. Jiménez, M. Sánchez, M. J. Zarzuelo, P. Galindo, A. M. Quintela, R.
619 López-Sepúlveda, M. Romero, J. Tamargo, F. Vargas, F. Pérez-Vizcaíno, J. Duarte,
620 Epicatechin lowers blood pressure, restores endothelial function, and decreases oxidative
621 stress and endothelin-1 and NADPH oxidase activity in DOCA-salt hypertension, *Free*
622 *Radic. Biol. Med.*, 2012, **52**, 70-79.
- 623 41 C. Boulanger, T. F. Lusher, Release of endothelin from the porcine aorta: inhibition by

- 624 endothelium-derived nitric oxide, *J. Chin. Inv.*, 1990, **85**, 587-590.
- 625 42 Y. Ushidaa, T. Matsuia, M. Tanakaa, K. Matsumotoa, H. Hosoyamab, A. Mitomib, Y.
626 Sagesakab, T. Kakuda, Endothelium-dependent vasorelaxation effect of rutin-free tartary
627 buckwheat extract in isolated rat thoracic aorta, *J. Nutr. Biochem.*, 2008, **19**, 700-707.
- 628 43 A. Larson, M. A. H. Witman, Y. Guo, S. Ives, R. S. Richardson, R. S. Bruno, T. Jalili, J. D.
629 Symons, Acute, quercetin-induced reductions in blood pressure in hypertensive individuals
630 are not secondary to lower plasma angiotensin-converting enzyme activity or endothelin-1:
631 nitric oxide, *Nutr. Res.*, 2012, **32**, 557-564.
- 632 44 Y. Cheng, S. C. Austin, B. Rocca, B. H. Koller, T. M. Coffman, T. Grosser, J. A. Lawson, G.
633 A. FitzGerald, Role of prostacyclin in the cardiovascular response to thromboxane A₂,
634 *Science*, 2002, **296**, 539-541.
- 635 45 Y. Shen, N. C. Ward, J. M. Hodgson, I. B. Puddey, Y. T. Wang, D. Zhang, G. J. Maghzal, R.
636 Stocker, K. D. Croft, Dietary quercetin attenuates oxidant-induced endothelial dysfunction
637 and atherosclerosis in apolipoprotein E knockout mice fed a high-fat diet: A critical role for
638 heme oxygenase-1, *Free Radic. Biol. Med.*, 2013, **65**, 908-915.
- 639 46 T. Choi, Y. Park, H. Choi, E. H. Lee, Anti-adipogenic activity of rutin in 3T3-L1 cells and
640 mice fed with high-fat diet, *Biofactors*, 2006, **26**, 273-281.
- 641 47 C. H. Jung, I. Cho, J. Ahn, T. I. Jeon, T. Y. Ha, Quercetin reduces high-fat diet-induced fat
642 accumulation in the liver by regulating lipid metabolism genes, *Phytother. Res.*, 2013, **27**,
643 139-143.
- 644 48 L. M. Tian, X. L. Shi, L. H. Yu, J. Zhu, R. Ma, X. B. Yang, Chemical composition and
645 hepatoprotective effects of polyphenol-rich extract from *Houttuynia cordata* tea, *J. Agric.*
646 *Food Chem.*, 2012, **60**, 4641-4648.
- 647 49 A. P. Rolo, J. S. Teodoro, C. M. Palmeira, Role of oxidative stress in the pathogenesis of
648 nonalcoholic steatohepatitis, *Free Radic. Biol. Med.*, 2012, **52**, 59-69.
- 649 50 X. S. Yang, C. A. Dong, G. X. Ren, Effect of soyasaponins-rich extract from soybean on

650 acute alcohol-induced hepatotoxicity in mice, *J. Agric. Food Chem.*, 2011, **59**, 1138-1144.

Figure Captions

Fig. 1. The HPLC chromatogram of purified tartary buckwheat flavonoid fraction (TBF, **A**) and standard flavonoids (**B**). Peaks: 1. Chlorogenic acid, 2. Caffeic acid, 3. Rutin, 4. Hypericin, 5. Quercetin, 6. Phloretin. HPLC analysis was carried out as described in the experimental section.

Fig. 2. Effects of TBF administration on plasma levels of NO (**A**) and eNOS (**B**), and serum levels of ET-1 (**C**), PGI₂ (**D**) and TX-A₂ (**E**) in the mice fed 1.5% high TMAO water for 8 consecutive weeks. Data are expressed as means ± SD for 10 mice in each group. ^{##} $p < 0.01$, vs the normal group. * $p < 0.05$, ** $p < 0.01$, compared to the TMAO group.

Fig. 3. Photomicrographs of aorta morphology. (**A**) Representative histological section of the aorta was stained by H&E (magnification 400 ×). The medial area was determined by the internal elastic lamina and external elastic lamina (arrows) and analyzed with image pro-plus 6.0 software. (**B**) Inhibitory effects of dietary supplementation of TBF on the wall thickness ratio (intimal area/media area) in mouse aorta. Data denoted are means ± SD (n = 10). ^{##} $p < 0.01$, vs the normal group. * $p < 0.05$, ** $p < 0.01$, compared to the TMAO group.

Fig. 4. Effects of TBF on activities of serum ALT (**A**) and AST (**B**) of high TMAO diet-fed mice for 8 consecutive weeks. Values are expressed as means ± SD of 10 mice in each group. ^{##} $p < 0.01$, vs the normal mice. * $p < 0.05$, ** $p < 0.01$, compared to TMAO-treated mice.

Fig. 5. Effects of TBF administration on hepatic levels of NEFA (**A**), MDA (**B**), T-SOD (**C**) and GSH-Px (**D**) in the mice fed 1.5% TMAO water for 8 consecutive weeks. Data are expressed as means ± SD for 10 mice in each group. ^{##} $p < 0.01$, vs the normal group. * $p < 0.05$, ** $p < 0.01$, compared to the TMAO-treated mice.

Fig. 6. Effects of TBF on histopathological changes of liver hepatocytes stained with H&E in high TMAO-fed mice (original magnification of 400 ×). (A) Normal group, (B) TMAO-treated mice, (C) TMAO + TBF (200 mg/kg·bw), (D) TMAO + TBF (400 mg/kg·bw), (E) TMAO + TBF (800 mg/kg·bw). The green arrows indicate normal cellular architecture with clear hepatic cell nucleus. The red arrows indicate the hepatic cell necrosis. The yellow arrows indicate the enlarged sinusoids between the plates of hepatocytes.

Fig. 7. Lipid staining of the liver section in mice (Oil and O staining, 400 ×). (A) Normal group, (B) TMAO-treated mice, (C) TMAO + TBF (200 mg/kg·bw), (D) TMAO + TBF (400 mg/kg·bw), (E) TMAO + TBF (800 mg/kg·bw).

Table 1

Effects of TBF on serum TC, TG, HDL-C and LDL-C levels of the mice fed high-TMAO diet for consecutive 8 weeks^a

Groups	TC	TG	HDL-C	LDL-C
	mmol/L			
Normal	3.01 ± 0.31	0.82 ± 0.13	0.94 ± 0.13	0.88 ± 0.14
TMAO	4.05 ± 0.62 ^{##}	1.53 ± 0.25 ^{##}	0.66 ± 0.10 ^{##}	1.19 ± 0.22 ^{##}
TMAO + TBF (200 mg/kg·bw)	3.92 ± 0.43	1.23 ± 0.26 [*]	0.82 ± 0.14	1.03 ± 0.19 [*]
TMAO + TBF (400 mg/kg·bw)	3.47 ± 0.76 [*]	1.02 ± 0.32 ^{**}	0.94 ± 0.17 ^{**}	0.96 ± 0.13 [*]
TMAO + TBF (800 mg/kg·bw)	3.27 ± 0.35 ^{**}	0.84 ± 0.45 ^{**}	1.02 ± 0.16 ^{**}	0.90 ± 0.14 ^{**}

^a Values are expressed as means ± SD of 10 mice in each group.

^{##} $p < 0.01$, as compared with the normal mice. ^{*} $p < 0.05$, ^{**} $p < 0.01$, compared to the TMAO-treated mice.

Table 2

Food Consumption, Water intake, Body weight, Liver weight, and Hepatosomatic index (HI) of mice at the end of week 8.

Groups	Food intake (g/d)	Water intake (ml/d)	Initial body wt (g)	Final body wt (g)	Liver wt (g)	HI (%)
Normal	10.29 ± 2.11	6.53 ± 2.16	28.10 ± 1.18	46.28 ± 2.76	2.04 ± 0.11	4.41 ± 0.28
TMAO	9.77 ± 1.68	6.34 ± 3.28	27.62 ± 1.21	48.97 ± 2.03 [#]	2.44 ± 0.15 ^{##}	4.97 ± 0.33 ^{##}
TMAO + TBF (200)	10.03 ± 1.34	6.47 ± 2.31	28.45 ± 0.77	47.74 ± 1.56	2.29 ± 0.17	4.80 ± 1.32
TMAO + TBF (400)	10.07 ± 1.98	6.36 ± 2.45	28.30 ± 1.46	46.61 ± 0.94 [*]	2.09 ± 0.15 ^{**}	4.48 ± 0.25 [*]
TMAO + TBF (800)	9.89 ± 1.57	6.32 ± 3.25	27.55 ± 0.92	46.39 ± 1.35 [*]	2.05 ± 0.17 ^{**}	4.42 ± 0.44 ^{**}

Values are expressed as means ± standard deviation of 10 mice in each group.

[#] $p < 0.05$, ^{##} $p < 0.01$, as compared with the normal group. ^{*} $p < 0.05$, ^{**} $p < 0.01$, compared to the TMAO-treated mice.

Fig. 1

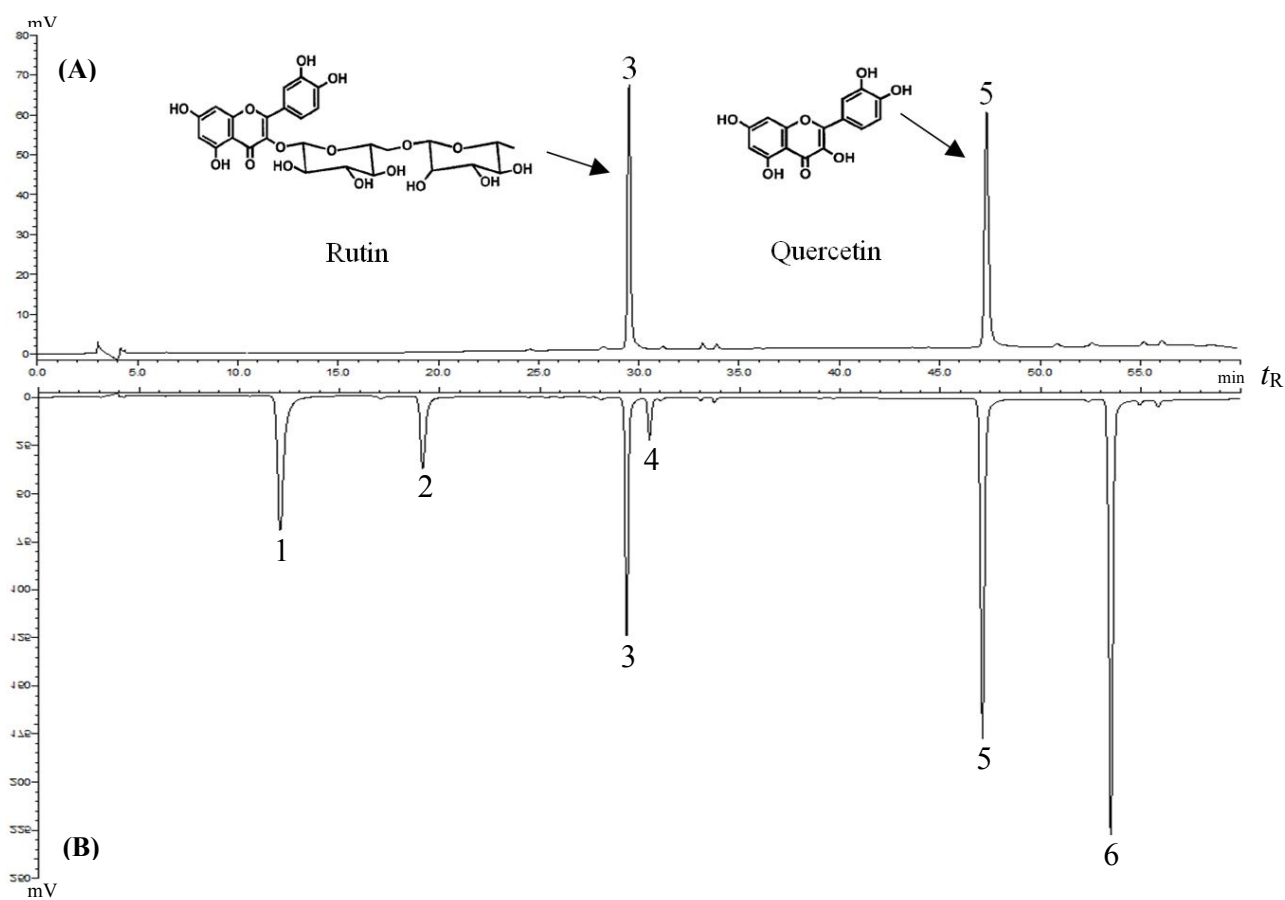


Fig. 2

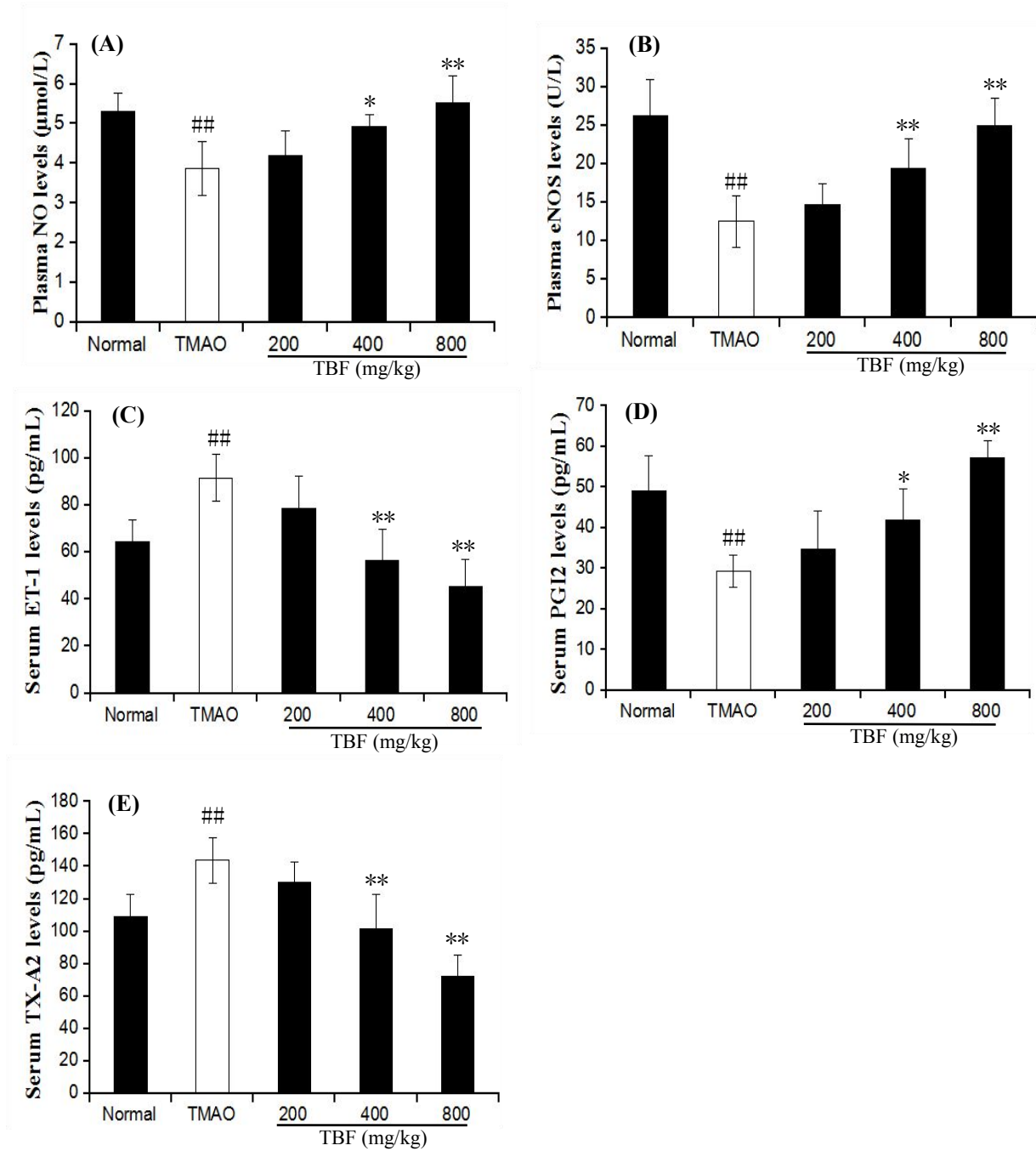


Fig. 3

(A)

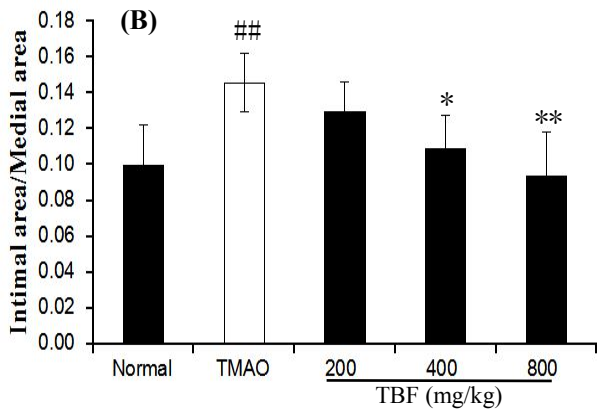
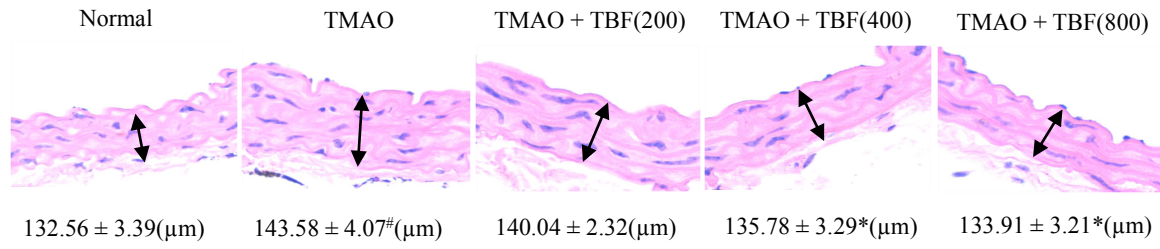


Fig. 4

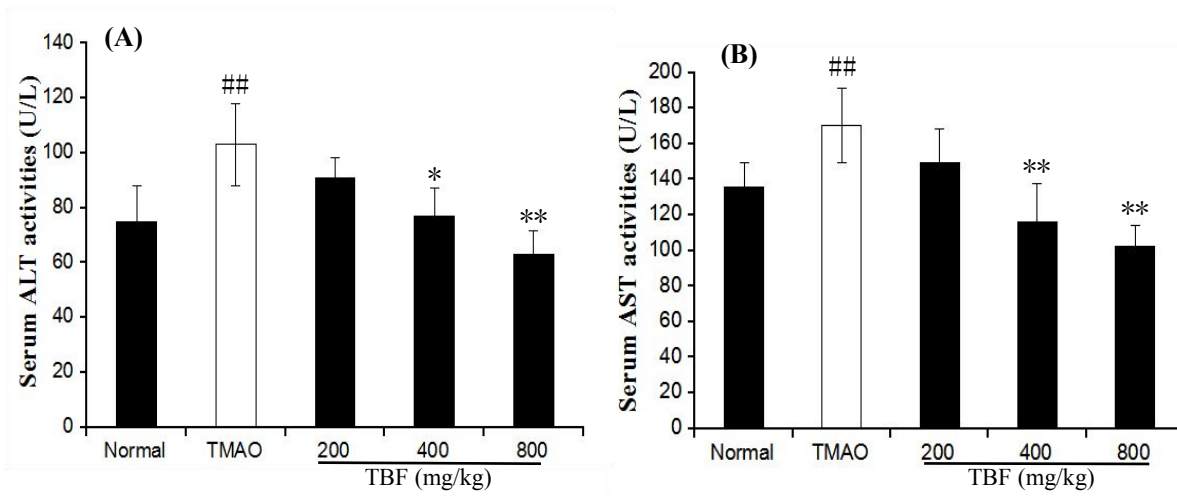


Fig. 5

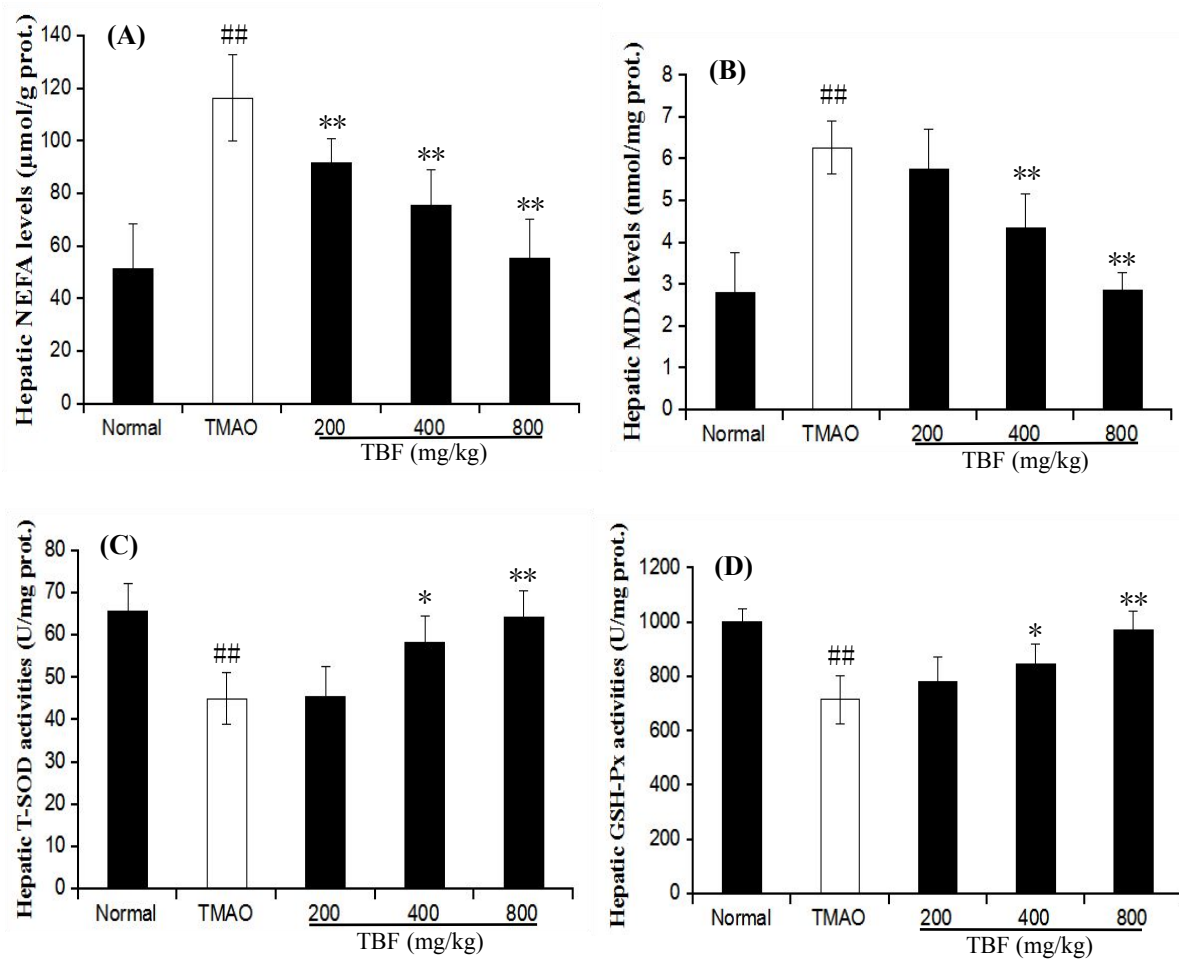
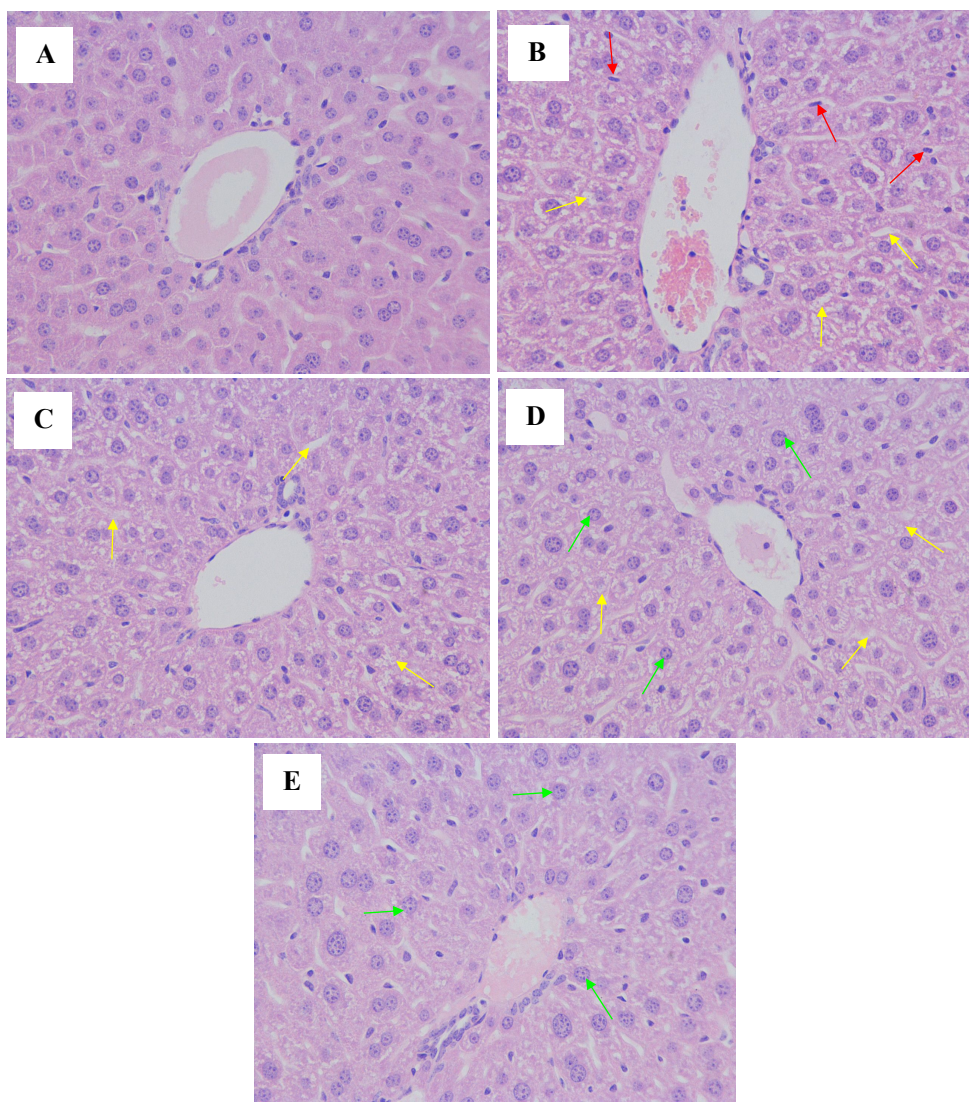
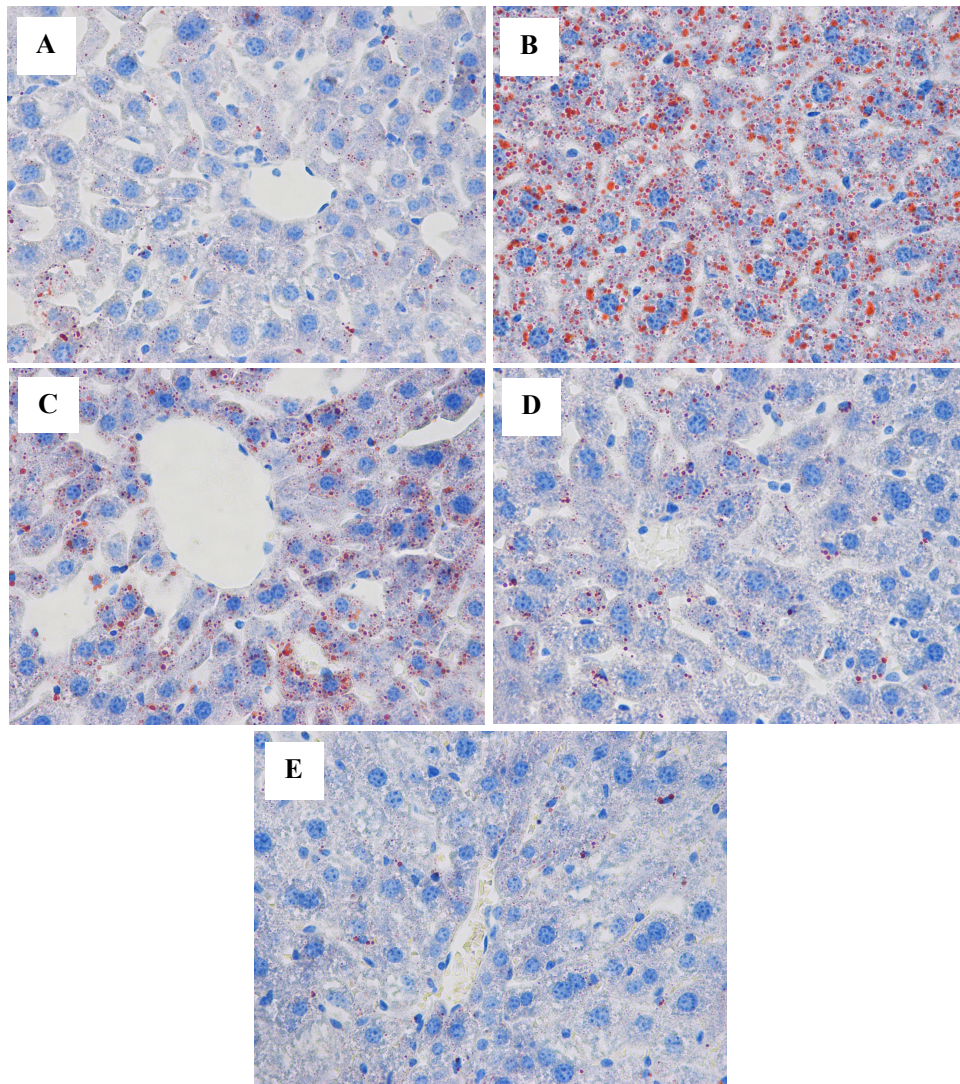


Fig. 6



Food & Function Accepted Manuscript

Fig. 7



TOC

